

Pedro Carmona · Marina Molina  
Arantxa Rodríguez-Casado

## Raman study of the thermal behaviour and conformational stability of basic pancreatic trypsin inhibitor

Received: 14 March 2002 / Revised: 5 December 2002 / Accepted: 5 December 2002 / Published online: 30 January 2003  
© EBSA 2003

**Abstract** We have studied the thermal denaturation of native basic pancreatic trypsin inhibitor (BPTI) by monitoring the Raman bands in the 4000–400  $\text{cm}^{-1}$  range. In agreement with results obtained by calorimetry, a cooperative melting transition is observed starting at 75 °C. This transition is found to involve predominantly the unfolding of helical structures accompanied by  $\beta$ -aggregation, loss of hydrophobic interactions between side chains and changes in CSSC dihedral angles. However, salt bridge breaking starts near 40 °C, as deduced from the  $\nu_s(\text{COO}^-)$  band and from the bands close to 1320 and 1345  $\text{cm}^{-1}$  which for the first time have been shown to be due largely to vibrations of the arginine guanidyl group in BPTI. The thermal stability is, hence, attributable to cooperative contributions from hydrophobic and backbone hydrogen bond interactions as well as from disulfide bonds.

**Keywords** Basic pancreatic trypsin inhibitor · Raman spectroscopy · Thermal stability

### Introduction

The recent discoveries of life at temperatures of 100 °C or higher have had increasing ramifications in biology

and biotechnology over the last decade (Stetter et al. 1990; Adams and Kallely 1992; Adams 1993). One of the fundamental questions arising from the study of hyperthermophilic organisms concerns the structural and energetic basis of protein stability at high temperatures, under conditions where many proteins from mesophilic organisms would be denatured. Thorough study of heat-stable proteins can reveal the structural determinants of heat stability at high temperatures.

Several studies have earlier been carried out to show the way proteins achieve heat stability (Chan et al. 1995; Vetriani et al. 1998; Wang et al. 1999; Kim et al. 2000). The attributes frequently proposed to explain this stability seem to be different from protein to protein, and they include a relatively small solvent-exposed surface area, an increased packing density that reduces cavities in the hydrophobic core, an increase of hydrophobicity in the core region, a decreased length of surface loops, disulfide bridges and increased hydrogen bonding between polar residues. Bovine pancreatic trypsin inhibitor (BPTI) is a small protein consisting of 58 amino acids, including three disulfide bridges. This protein is highly stable and very resistant toward denaturation, with its disulfides still remaining intact (Moses and Hinz 1983; Hurle et al. 1990; Makhatadze et al. 1993). To date, the majority of investigations of BPTI stability have applied the technique of reductive unfolding and focused on mutant molecules lacking one of the three disulfides (typically Cys14-Cys38) (Kress and Laskowski 1967; Marks et al. 1987; Goldenberg 1988; Li et al. 1995; Chang and Ballatore 2000). A systematic study of BPTI mutants showed that the mechanism of reductive unfolding of BPTI is consistent with its reversed pathway of oxidative folding, and also revealed that the stability of the disulfides in native BPTI depends on both the local environment and the rest of the protein to favour their formation (Goldenberg et al. 1993; Mendoza et al. 1994). On the other hand, some thermodynamic studies have attributed the stability of this protein to hydrogen bonding and van der Waals interactions (Makhatadze et al. 1993). It is known that the disruption of interactions

P. Carmona (✉)  
Instituto de Estructura de la Materia (CSIC),  
Serrano 121, 28006 Madrid, Spain  
E-mail: p.carmona@iem.cfm.csic.es  
Fax: +34-91-5645557

M. Molina  
Departamento de Química Orgánica I,  
Escuela Universitaria de Óptica,  
Arcos de Jalón s/n, 28037 Madrid, Spain

A. Rodríguez-Casado  
Department of Crystallography,  
Birbeck College, University of London, Malet Street,  
Bloomsbury, London, WC1E 7HX, UK

between the side chains is necessary for protein denaturation, but it does not necessarily lead to extensive unfolding of the polypeptide backbone (Chan et al. 1995; Vetriani et al. 1998; Wang et al. 1999; Kim et al. 2000). The heat-induced denaturation of proteins may not necessarily be accompanied by extensive unfolding of the protein backbone. The nature of heat-induced denaturation of BPTI is still not well understood, and detailed characterization of the BPTI secondary structure, as well as of tertiary structural details, upon heat-induced denaturation is essential to our understanding of its mechanism.

In this paper, we report a thermal denaturation study of BPTI by Raman spectroscopy. Vibrational spectroscopy has emerged as a valuable tool for following conformational changes in proteins and can separately monitor substructures within the intact proteins and also be sensitive to fast interchanging forms. Thus, it has been shown that helices, the  $\beta$ -structure and the disordered backbone could be determined separately from the Raman spectra of proteins in the amide I region (Williams and Dunker 1981; Tu 1982; Williams 1983; Krim and Bandekar 1986; Alix et al. 1988). In addition, some details of protein tertiary structure (environment of tyrosine side chain, disulfide bridge conformations, hydrophobic contacts, salt bridges) can be revealed by this technique (Overman and Thomas 1998a, 1998b, 1999; Tsuboi et al. 2000). In this connection, we have used model compounds such as the L-arginine L-glutamate salt and L-leucine methyl ester for studying the spectral features of carboxylate-guanidyl salt bridges and hydrophobic contacts, respectively. The use of these model compounds is supported by the fact that the vibrational motions of carboxyl and guanidyl groups are very localized in these atomic groupings (Tu 1982; Nakamoto 1997). Similarly, it is well known that the hydrocarbon side chain of L-leucine generates vibrations which are very localized in this hydrocarbon moiety (Tu 1982). On this basis it seems reasonable that the spectral behaviour inherent in formation or breaking of carboxylate-guanidyl salt bridges and hydrophobic contacts does not depend on the molecules where these atomic groupings are present, and consequently they can be characterized through the above model compounds. Accordingly, the heat dependence of the BPTI secondary and tertiary structures has been followed by Raman spectroscopy to determine the roles of the above structural details in the heat stability of BPTI.

## Materials and methods

### Materials

BPTI from bovine lung was purchased from Calbiochem and used without further purification. BPTI purity was checked by SDS-PAGE and was found to be greater than 98%. L-Leucine methyl ester hydrochloride (LMEH) and L-arginine L-glutamate salt (AGS) were obtained from Sigma in the highest available grade (purity greater than 99%).

### Raman spectroscopy

Solutions of BPTI were prepared at 80 mg mL<sup>-1</sup> in 50 mM sodium cacodylate buffer (pH 6.5). Samples were sealed in standard glass capillaries for Raman analysis and measured in a temperature-controlled home-made device. The temperature was controlled within 0.3 °C by a circulating water jacket. FT Raman spectra were excited at 1064 nm with a Nd:YAG laser and recorded on a computer-controlled Bruker RFS 100/S FT spectrometer. The Raman scattered was collected at 180° to the source and analysed with 4 cm<sup>-1</sup> spectral resolution. Frequencies cited are accurate to  $\pm 0.3$  cm<sup>-1</sup>, and each spectrum of high signal-to-noise ratio was obtained after collecting and averaging 2000 scans measured with 200 mW of laser power at the sample. Signals obtained were fed to a microcomputer for storage, display, plotting and processing, and the manipulation and evaluation of the spectra were carried out through the SpectraCalc software (Galactic Industries, Salem, NH, USA). Linear baseline corrections were performed on the spectra in order to facilitate intensity comparisons. In all cases, the buffer was compensated by computer subtraction techniques (Williams 1983; Benevides et al. 1984) and removing the 608 cm<sup>-1</sup> strong band of the buffer used as internal standard. In this connection, the spectrum of the aqueous buffer was always recorded with the same instrument settings employed for protein solutions.

The aqueous solution Raman spectra of LMEH and AGS were measured at 0.2–2 M concentrations, using the above buffer and spectroscopic conditions. Normalized spectra were compared by digital difference methods using the above software. The positive and negative difference bands were measured from the flat baseline established by connecting the common points of zero Raman intensity (minima between bands) in the constituent spectra. We have used the following criteria for selection and discussion of peaks and troughs in the difference spectra. Firstly, a difference band should exhibit an intensity ratio at least twofold that of the experimental noise level shown in the 1800–1700 cm<sup>-1</sup> range. Secondly, the difference feature should not be affected by baseline or solvent corrections and must be reproducible for independently prepared samples. Lastly, the difference band must be structurally interpretable.

Protein secondary structures were determined as percentages of  $\alpha$ ,  $\beta$ , turn and unordered conformations (Williams 1983; Alix et al. 1988). With this aim, the water spectrum was previously subtracted from the spectra by following the same criteria as those described in the literature (Williams and Dunker 1981; Williams 1983). Assignment of the visible bands to vibrational modes of peptide backbone or amino acid side chains was carried out through comparison with Raman spectra of model polypeptides or monographs of Raman spectra of proteins (Tu 1982; Krim and Bandekar 1986; Overman and Thomas 1998a, 1998b, 1999; Tsuboi et al. 2000).

## Results and discussion

### Secondary structure

The spectra of BPTI in aqueous solution at different temperatures are shown in Fig. 1. The amide I band, which is located in the 1700–1600 cm<sup>-1</sup> region, shows at 25 °C an intensity maximum at 1665 cm<sup>-1</sup> (Fig. 1A). The frequency of this band is consistent with the presence of a major proportion of unordered structure in the protein (Wagner et al. 1987), as the amide I 1668–1660 cm<sup>-1</sup> range is attributable to this type of protein secondary structure (Tu 1982). At temperatures above 80 °C a band located at 1674 cm<sup>-1</sup> increases in intensity, which is unambiguously assigned to  $\beta$ -sheets on the basis that proteins containing relatively high amounts of this

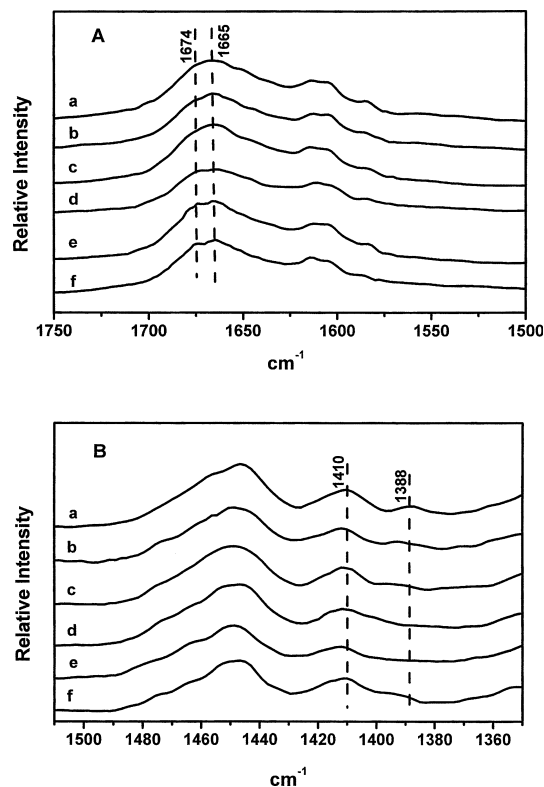


**Fig. 1A, B** Raman spectra of 12 mM BPTI in 50 mM sodium cacodylate buffer (pH 6.5) at 25, 45, 60, 80 and 95 °C (from *a* to *e*), and at 25 °C after heating at 95 °C for 5 min (*f*). **A** 1750–1500  $\text{cm}^{-1}$  region; **B** 1510–1350  $\text{cm}^{-1}$  region

backbone structure exhibit bands in the 1680–1670  $\text{cm}^{-1}$  range (Tu 1982; Krim and Bandekar 1986). Heating up to 95 °C and subsequent cooling at 25 °C generates a spectrum revealing that  $\beta$ -sheet structure concentration generated at 95 °C does not change significantly after reaching 25 °C (Fig. 1A, Table 1), which means that irreversible denaturation occurs to some extent. Within the 25–75 °C temperature range, no significant changes in secondary structure were observed (Fig. 2). However,  $\alpha$ -helices transform into  $\beta$ -sheets, turns and unordered structures above 75 °C. These spectral changes correspond to the cooperative unfolding transition occurring between 80 and 110 °C, detected by calorimetry (Hansen et al. 1998), whose temperature top endothermic peak is

**Table 1** Raman determination of protein secondary structures in BPTI

Temperature (°C)	$\alpha$ -Helices	$\beta$ -Sheets	Turns	Unordered
25	26 $\pm$ 2	27 $\pm$ 1	7 $\pm$ 0.5	40 $\pm$ 3
80	23 $\pm$ 2	30 $\pm$ 1	8 $\pm$ 1	39 $\pm$ 2
95	8 $\pm$ 1	38 $\pm$ 2	9 $\pm$ 1	45 $\pm$ 2
25 <sup>a</sup>	16 $\pm$ 2	38 $\pm$ 2	8 $\pm$ 1	38 $\pm$ 2
25 <sup>b</sup>	25	27	7	41

<sup>a</sup>Values obtained from BPTI solution at 25 °C after heating at 95 °C for 30 min

<sup>b</sup>Values obtained from Robertson and Murphy (1997)

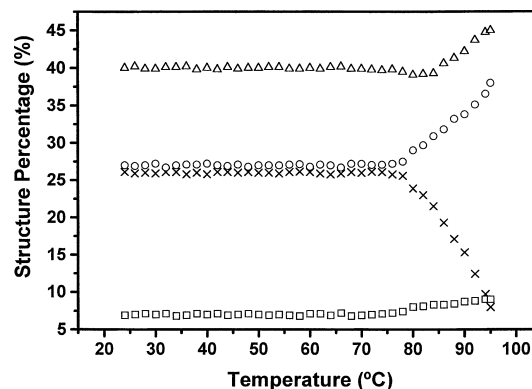


**Fig. 2** BPTI secondary structure percentages versus temperature:  $\alpha$ -helix (crosses),  $\beta$ -sheet (circles), turns (squares) and unordered (triangles)

located at 95 °C. Cooling to 25 °C allows the protein to recover part of the native  $\alpha$ -helices, but a  $\beta$ -sheet excess still remains (Table 1) due to protein aggregation. This incomplete reversibility of unfolding of BPTI was also observed by calorimetry (Makhatadze et al. 1993). Generally speaking, heat-resistant proteins, such as BPTI, have extremely high  $T_m$  values (near or above water boiling point). However, when the temperature is at or above  $T_m$ , most heat-resistant proteins also denature, leading to insoluble aggregation (Kim et al. 2000).

### Charged side chains and salt bridging

From the spectra included in Fig. 1B, it can be seen that the frequencies of the 1410 and 1388  $\text{cm}^{-1}$  bands, attributable to the  $\nu_s(\text{COO}^-)$  vibrational mode, upshift with increasing temperature. Unlike the BPTI secondary structure, these frequency changes can be observed above 40 °C. This can be interpreted in terms of salt bridge disruption with increasing temperature. In fact, it is well established that  $\nu_s(\text{COO}^-)$  bands shift to higher frequencies as the interactions of  $\text{COO}^-$  groups with their oppositely charged partners weaken (Nakamoto 1997). The solution structure of BPTI that could be studied by NMR (Wagner et al. 1987) involves intramolecular salt bridges on the protein surface. These salt bridges are between the side chains of Asp50 and Lys46, the side chains of Glu7 and Arg42 and the side chain of Arg1 and the carboxyl terminus of Ala58. The above temperature-dependent frequency changes of the 1410 and 1388  $\text{cm}^{-1}$  bands are likely due to varying strengths of these salt bridges. In support of this are also the spectral profiles in the 1350–1300  $\text{cm}^{-1}$  range (Fig. 3A). With increasing temperature, one can notice weakening of the band near 1343  $\text{cm}^{-1}$  and frequency upshifting of the band located at 1321  $\text{cm}^{-1}$ . These spectral changes can be attributed to salt bridges where the arginine residues take part. This assignment has been achieved by examining the spectra of arginine glutamate (AGS), in which concentration-dependent gradual joining of

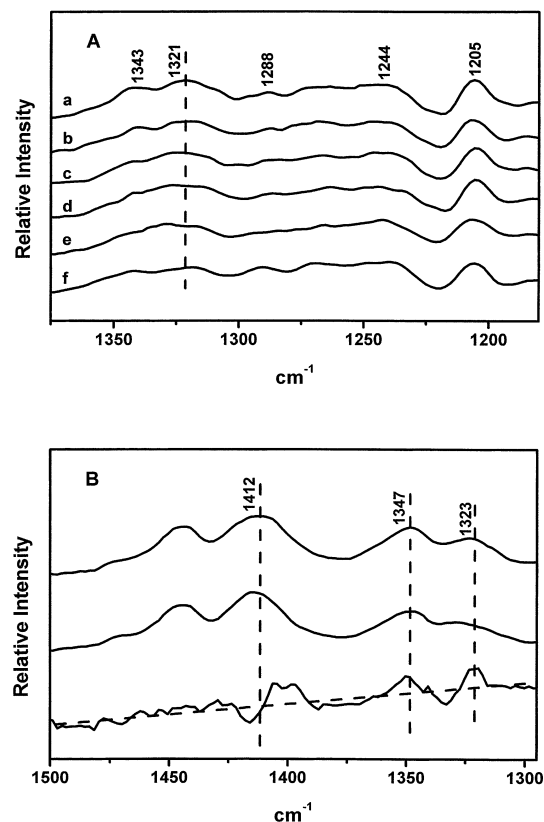


**Fig. 3** **A** Raman spectra (1375–1175  $\text{cm}^{-1}$  region) of 12 mM BPTI in 50 mM sodium cacodylate buffer (pH 6.5) at 25, 45, 60, 80 and 95 °C (from *a* to *e*), and at 25 °C after heating at 95 °C for 5 min (*f*). **B** Normalized Raman spectra of 1.5 M AGS (*upper*), 0.03 M AGS (*middle*) and five-fold amplified difference spectrum between 1.5 M AGS and 0.03 M AGS (*lower*)

oppositely charged groups can be studied systematically (Fig. 3B). The normalized spectra of AGS show the following behaviour with decreasing AGS concentration: shifting of the  $\nu_s(\text{COO}^-)$  band (1412  $\text{cm}^{-1}$ ) towards higher frequencies, and intensity decrease and frequency upshifting of the 1347 and 1323  $\text{cm}^{-1}$  bands, respectively. These concentration-dependent spectral changes can be explained by considering that the proportion of direct contacts (salt bridges) between  $\text{COO}^-$  groups and the positively charged guanidyl group of arginine decreases with decreasing concentration. On this basis, frequency upshifting of the  $\nu_s(\text{COO}^-)$  band is expected upon dilution, for the same structural reason as that described above concerning the spectral behaviour of this band versus temperature. As to the 1347 and 1323  $\text{cm}^{-1}$  bands, these have been assigned respectively to  $\delta(\text{CH})$  and  $\nu(\text{C-N})$  vibrations of charged arginine side chains (Dhanaraj et al. 1991; Braiman et al. 1999). In the mesomeric state of the arginine guanidyl group, the C-N bonds acquire partial double-bond character (Angell et al. 1957). This means that the stronger the linking of the guanidyl group to the  $\text{COO}^-$  group (salt bridge formed at high AGS concentrations), the greater the loosening of the proton from the charged guanidyl

group, whereby the C-N bonds acquire more single-bond character and their frequency near 1325  $\text{cm}^{-1}$  hence decreases.

In previous publications dealing with assignments of protein Raman bands, it was shown that an  $\alpha$ -helical main chain generates a medium intensity band near 1343  $\text{cm}^{-1}$  due to a vibration involving both C-C $\alpha$ -H valence angle bending and C-C $\alpha$  stretching (Overman and Thomas 1998a, 1998b, 1999). Although in  $\alpha$ -helix-rich proteins this band can be regarded as an empirical marker of the main-chain C $\alpha$ H groups and may be  $\alpha$ -helical conformational dependent (Overman and Thomas 1998a, 1998b, 1999), the proportion of  $\alpha$ -helices in BPTI is relatively low (Table 1) for this band (Fig. 3A) to be considered a major contribution from the  $\alpha$ -helical backbone. Moreover, its gradual disappearance in the spectra of BPTI with increasing temperature cannot be attributed to a concomitant diminution of  $\alpha$ -helices, because the amide I band profiles reveal that this transition occurs above 75 °C (Fig. 2). Consequently, the temperature-dependent spectral changes observed for this 1343  $\text{cm}^{-1}$  band can be unambiguously assigned to the salt bridges involving arginine residues, which are among the most abundant residues (10.3%) in BPTI (Wagner et al. 1987). Moreover, the intensity and frequency of this band is altered upon deuteration, and it is not due to the Trp residue because this amino acid is not present in the BPTI molecule (Wagner et al. 1987). The above unambiguous assignment to the arginine residue is also supported by the fact that in the aqueous solution spectra of AGS (Fig. 3B) there is also a band near 1345  $\text{cm}^{-1}$  whose intensity decreases upon increasing temperature and concomitant breaking of the carboxylate-guanidyl salt bridges that are formed at high AGS concentrations. On the other hand, although the 1321  $\text{cm}^{-1}$  band of BPTI (Fig. 3A) may result from extensive overlapping of several nonaromatic side-chain vibrations (CH<sub>2</sub> twist/rock) (Overman and Thomas 1999), contribution of the arginine guanidyl group is great, as reflected by the above-mentioned frequency shifting versus temperature due to hydrogen bonding changes. All of these results reveal that in proteins whose  $\alpha$ -helical content is relatively low, as occurs in BPTI, salt bridges involving arginine residues can be detected in Raman spectra.

#### Hydrophobic interactions and disulfide bridges

Figure 4A shows the C-H stretching region of the Raman spectra of BPTI at varying temperatures. Increasing intensity and a shift in the location of the peak intensity from 2933 to 2937  $\text{cm}^{-1}$  was observed in going from 25 °C to 95 °C. Published data are scarce for this C-H stretching band in protein spectra. Some authors (Careche and Li-chan 1997; Howell et al. 1999) reported a slight shift to higher frequencies when urea was added to aqueous buffered solutions. Those results suggest partial unfolding and increased exposure of the

aliphatic residues to an aqueous environment. In support of this are the spectra of LMEH scanned at 0.1 and 2 M concentrations, which presumably contain different proportions of hydrophobic contacts (Fig. 4B). The spectrum of 2 M LMEH shows three bands at 2966, 2934 and 2877  $\text{cm}^{-1}$  generated by C-H stretching motions of the  $\text{CH}_3$  and  $\text{CH}_2$  groups. In going from the 2 M LMEH spectrum to the normalized spectrum of 0.1 M LMEH, part of the hydrophobic interactions are lost and this results in concomitant frequency upshifts of the above bands. These frequency changes are accompanied by decreasing intensity of the 2966 and 2934  $\text{cm}^{-1}$  bands.

All of these results are consistent with loosening of the hydrophobic contacts in BPTI at high temperatures (above 80 °C), these being slightly above those causing the structural changes of the BPTI secondary structure.

The very well-known intensity ratio ( $I_{856}/I_{828}$ ) of the band components in the Fermi doublet of tyrosine is 1.25, which is diagnostic for a tyrosine hydroxyl group acting as both donor and acceptor of moderate hydrogen bonds, for instance, when exposed to solvent water molecules (Overman et al. 1994). The above intensity

ratio does not change significantly with the temperature of BPTI solutions, even when heated at 95 °C.

Disulfide bridges are important elements of protein primary sequence that add to the stability of the entire BPTI molecular structure (Chang and Ballatore 2000). In the Raman spectrum of BPTI in aqueous solution, a medium intensity band for disulfide bridges appears at 511  $\text{cm}^{-1}$  (Fig. 5), which is indicative of a g-g-g conformation of the CCSSCC dihedral angles adopted by naturally occurring proteins and peptides (Sugeta 1973; Sugeta et al. 1973; Tuma et al. 1995). Other bands occasionally observed for peptides and proteins are located between 600 and 700  $\text{cm}^{-1}$  due to C-S stretching vibrations, but in BPTI they appear with very weak intensity and are not suitable to monitor conformational transitions of the CCSSCC dihedral angles. It was found by Sugeta et al. (1973) that the stretching vibration of the disulfide bond is influenced by the conformation of the carbon atoms in the CCSSCC disulfide bridge, and the band near 510  $\text{cm}^{-1}$  can be assigned to the g-g-g conformation. The covalently linked disulfide bridges in BPTI are not broken by heat treatment up to 95 °C, as the S-S stretching intensity does not decrease over this temperature range. However, a frequency shift from 511 to 506  $\text{cm}^{-1}$  is observed in going from 25 to 95 °C, suggesting that there are changes in the geometry of the CSSC dihedral angles. These changes occur above 75 °C.

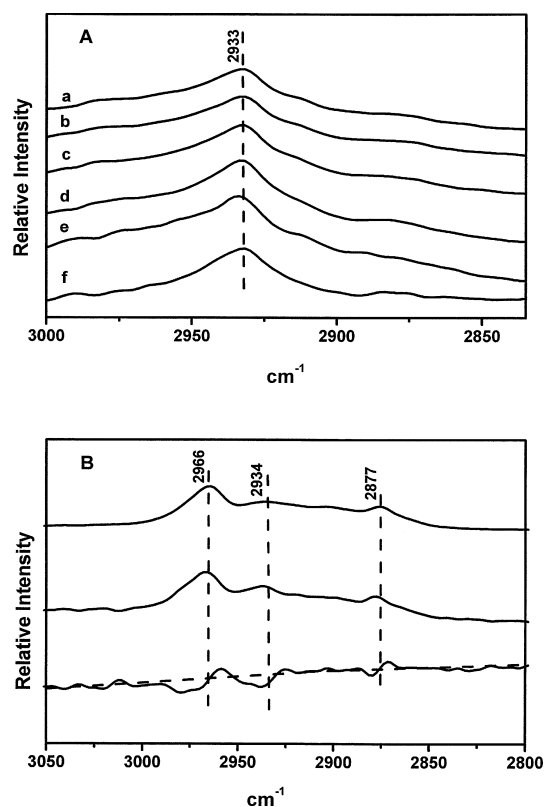


**Fig. 4** A Raman spectra (3000–2835  $\text{cm}^{-1}$  region) of 12 mM BPTI in 50 mM sodium cacodylate buffer (pH 6.5) at 25, 45, 60, 80 and 95 °C (from a to e), and at 25 °C after heating at 95 °C for 5 min (f). B Normalized Raman spectra of 2 M LMEH (upper), 0.1 M LMEH (middle) and a three-fold amplified difference spectrum between 2 M LMEH and 0.1 M LMEH (lower)

### Thermal stability of BPTI

A characteristic property of this enzyme is the great thermal stability of the structure. An assessment of the origins of this stability must necessarily be based on the analysis of the above spectroscopic results and of rather general features of protein structure and stability established primarily from heat-labile proteins.

Factors affecting the stability of proteins, such as salt bridge formation, have attracted much interest (Hansen

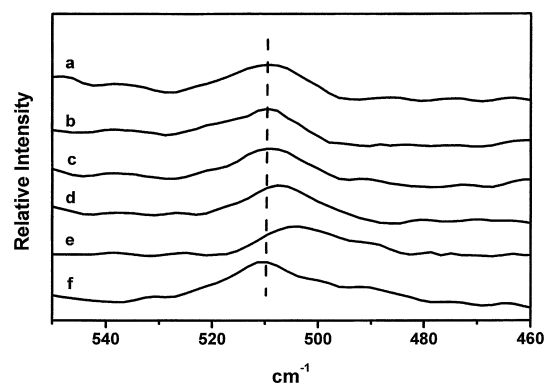


**Fig. 5** Raman spectra (550–460  $\text{cm}^{-1}$  region) of 12 mM BPTI in 50 mM sodium cacodylate buffer (pH 6.5) at 25, 45, 60, 80 and 95 °C (from a to e), and at 25 °C after heating at 95 °C for 5 min (f)

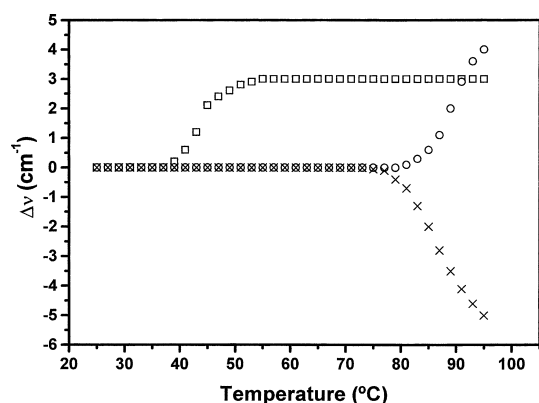


**Fig. 6** Frequency shifts (relative to 25 °C) for the  $\nu_s(\text{COO}^-)$  (squares),  $\nu(\text{CH})$  (circles) and  $\nu(\text{SS})$  (crosses) bands of 12 mM BPTI, in 50 mM sodium cacodylate buffer (pH 6.5), versus temperature

et al. 1998), although some studies have questioned the significance of the contributions of these interactions to protein stability (Dao-pin et al. 1991; Hendsch and Tidor 1994). Our spectroscopic results reveal (Fig. 6) that BPTI salt bridges are labile above 40 °C, and consequently do not contribute significantly to the high resistance to BPTI denaturation by temperature. These results are consistent with the fact that the BPTI salt bridges are located on the protein surface (Wagner et al. 1987), and in these conditions the contribution to stability from each salt bridge is very small (about 0.1–0.25 kcal/mol) (Dao-pin et al. 1991). Owing to the low heat effect accompanying the BPTI salt bridge breaking, this transition was not detectable by differential scanning calorimetry (Makhatadze et al. 1993).

The secondary structure composition of BPTI (26% helix, 23%  $\beta$ -sheet) (Table 1) is within the range seen for water-soluble globular proteins. Thus, while the secondary structure disruption of BPTI occurs above 75 °C (Fig. 2) and, hence, the ordered backbone structure may contribute to the stability of this protein, this structural feature cannot represent the sole determinant of thermostability. The stability of BPTI stands out among numerous disulfide-containing proteins. Concerning their relative stability, defined by the concentration of denaturants required to denature 50% of the protein, BPTI exhibits total resistance against 3.25 M guanidine thiocyanate, and ribonuclease A is fourfold less stable than BPTI (Chang and Ballatore 2000). However, the number of disulfide bridges per residue is 0.051 and 0.032 in BPTI and ribonuclease A, respectively. Therefore, it seems obvious that the BPTI stability cannot depend on the disulfide bridges alone.

All of the above spectroscopic results and thermodynamic data suggest the cooperative nature of interactions in BPTI and that the stability of this protein may reflect a number of subtle interactions leading to other features of protein structure. Thus, other attributes frequently proposed to explain the heat stability

of proteins include a relatively small solvent-exposed surface area and increased packing density that reduces cavities in the hydrophobic core (Kim et al. 2000). The possibility that minimization of the molecular surface-area-to-volume ratio might contribute to the stability of BPTI has been assessed here by evaluating the relative surface area ( $SA_R$ ) and the fraction of buried atoms ( $n_B$ ) in the BPTI molecule. By following literature methods (Chotia 1975; Chan et al. 1995), we have evaluated these two parameters for BPTI, which were found to be 0.71 ( $SA_R$ ) and 0.60 ( $n_B$ ). These values are near those obtained for the aldehyde ferredoxin oxidoreductase (AOR) (0.83 for  $SA_R$  and 0.56 for  $n_B$ ), which is a very thermostable enzyme (Chan et al. 1995). Consequently, rather than being the consequence of one dominant type of interaction, it appears that the thermal stability of BPTI reflects that hydrogen bonds, hydrophobic interactions and disulfide bridges cooperatively contribute to minimize the molecular surface energy while maximizing packing interactions.

In conclusion, the thermal denaturation of BPTI has been first monitored by Raman spectroscopy. According to previous calorimetry studies, a cooperative melting transition starts near 75 °C which involves predominantly unfolding of  $\alpha$ -helices and  $\beta$ -aggregation, loss of hydrophobic interactions between side chains and changes in CSSC disulfide torsion angles. However, salt-bridge breaking starts near 40 °C, as shown by the spectral behaviour of the  $\nu_s(\text{COO}^-)$  band and the behaviour of the bands near 1345 and 1320  $\text{cm}^{-1}$ , which for the first time are shown to be generated largely by guanidyl group motions in arginine residues. Thus, in arginine-rich proteins, such as BPTI, these bands can be exploited as a novel indicator of salt-bridge formation/breaking involving arginine residues. Taking into account the temperatures where the different types of intra- and intermolecular bonds start breaking, the thermal stability of BPTI is attributable to cooperative contributions from hydrophobic and protein backbone hydrogen-bond interactions as well as from disulfide bridges, all of these interactions leading to minimize the solvent-exposed surface area while maximizing packing density.

**Acknowledgements** We are grateful to Dirección General de Investigación, Comunidad Autónoma de Madrid, for financial support (project 07G/0053/2000).

## References

- Adams MWW (1993) Enzymes and proteins from organisms that grow near and above 100 °C. *Annu Rev Microbiol* 47:627–658
- Adams MWW, Kalley RM (1992) Biocatalysis at extreme temperatures: enzyme systems near and above 100 °C. *ACS Symp Ser* 498:1
- Alix AJP, Pedanou G, Berjot M (1988) Fast determination of the quantitative secondary structure of proteins by using some parameters of the Raman amide I band. *J Mol Struct* 174:159–164

- Angell CL, Sheppard N, Yamaguchi A, Shimanouchi T, Miyazawa T, Mizushima S (1957) The infrared spectrum, structure, and normal vibrations of the guanidinium ion. *Trans Faraday Soc* 53:589–600
- Benevides JM, Wang AHJ, van der Marel GA, van Boom JH, Rich A, Thomas GJ Jr (1984) The Raman spectra of left-handed DNA oligomers incorporating AT base pairs. *Nucleic Acids Res* 12:5913–5925
- Braiman MS, Briercheck DM, Kriger KM (1999) Modeling vibrational spectra of amino acid side chains in proteins: effects of protonation state, counterion, and solvent on arginine C-N stretch frequencies. *J Phys Chem B* 103:4744–4750
- Careche M, Li-chan E (1997) Structural changes in cod myosin after modification with formaldehyde or frozen storage. *J Food Sci* 62:717–723
- Chan MK, Mukund S, Kletzin A, Adams MWW, Reeds DC (1995) Structure of a hyperthermophilic tungstopterin enzyme, aldehyde ferredoxin oxidoreductase. *Science* 267:1463–1469
- Chang JY, Ballatore A (2000) The structure of denatured bovine pancreatic trypsin inhibitor (BPTI). *FEBS Lett* 473:183–187
- Chotia C (1975) Structural invariants in protein folding. *Nature* 254:304–308
- Dao-pin S, Sauer U, Nicholson H, Matthews BW (1991) Contributions of engineered surface salt bridges to the stability of T4 lysozyme determined by directed mutagenesis. *Biochemistry* 30:7142–7153
- Dhanaraj G, Srinivasan MR, Bhat HL (1991) Vibrational spectroscopic study of L-arginine phosphate monohydrate (LAP). A new organic non-linear crystal. *J Raman Spectrosc* 22:177–181
- Goldenberg DP (1988) Kinetic analysis of the folding and unfolding of a mutant form of bovine pancreatic trypsin inhibitor lacking the cysteine-14 and -38 thiols. *Biochemistry* 27:2481–2489
- Goldenberg DP, Bekeart LS, Laheru DA, Zhou JD (1993) Probing the determinants of disulfide stability in native pancreatic trypsin inhibitor. *Biochemistry* 32:2835–2844
- Hansen PE, Zhang W, Lauritzen C, Bjørn S, Petersen LC, Norris K, Olsen OH, Betzel C (1998)  $^{13}\text{C}$  NMR, X-ray, and differential scanning calorimetry investigations of truncated BPTI (aprotinin) analogues. *Biochemistry* 37:3645–3653
- Hendsch ZS, Tidor B (1994) Do salt bridges stabilize proteins? A continuum electrostatic analysis. *Protein Sci* 3:211–226
- Howell NK, Arteaga G, Nakai S, Li-chan EY (1999) Raman spectral analysis in the C-H stretching region of proteins and amino acids for investigation of hydrophobic interactions. *J Agric Food Chem* 47:924–933
- Hurle MR, Marks CB, Kosen PA, Anderson S, Kuntz ID (1990) Denaturant-dependent folding of bovine pancreatic trypsin inhibitor mutants with two intact disulfide bonds. *Biochemistry* 29:4410–4419
- Kim TD, Ryu HJ, Cho HI, Yang CH, Kim J (2000) Thermal behavior of proteins: heat resistant proteins and their heat-induced secondary structural changes. *Biochemistry* 39:14839–14846
- Kress LF, Laskowski M Sr (1967) The basic trypsin inhibitor of bovine pancreas. VII. Reduction with borohydride of disulfide bond linking half-cystine residues 14 and 38. *J Biol Chem* 242:4925–4929
- Krim S, Bandekar (1986) Vibrational spectroscopy and conformation of peptides, polypeptides, and proteins. *Adv Protein Chem* 38:181–364
- Li YJ, Rothwart DM, Scheraga HA (1995) Mechanism of reductive protein unfolding. *Nat Struct Biol* 2:489–494
- Makhatadze GI, Kim KS, Woodward C, Privalov PL (1993) Thermodynamics of BPTI folding. *Protein Sci* 2:2028–2036
- Marks CB, Naderi H, Kosen PA, Kuntz ID, Anderson S (1987) Mutants of bovine pancreatic trypsin inhibitor lacking cysteines 14 and 38 can fold properly. *Science* 235:1370–1373
- Mendoza JA, Jarstfer MB, Goldenberg DP (1994) Effects of amino acid replacements on the reductive unfolding kinetics of pancreatic trypsin inhibitor. *Biochemistry* 33:1143–1148
- Moses E, Hinz HJ (1983) Basic pancreatic trypsin inhibitor has unusual thermodynamic stability parameters. *J Mol Biol* 170:765–776
- Nakamoto K (ed) (1997) Infrared and Raman spectra of inorganic and coordination compounds. Part B. Applications in coordination, organometallic, and bioinorganic chemistry. Wiley, New York, chap 4
- Overman SA, Thomas GJ Jr (1998a) Novel vibrational assignments for proteins from Raman spectra of viruses. *J Raman Spectrosc* 29:23–29
- Overman SA, Thomas GJ Jr (1998b) Amide modes of the  $\alpha$ -helix: Raman spectroscopy of filamentous virus Fd containing peptide  $^{13}\text{C}$  and  $^2\text{H}$  labels in coat protein subunits. *Biochemistry* 37:5654–5665
- Overman SA, Thomas GJ Jr (1999) Raman markers of nonaromatic side chains in an  $\alpha$ -helix assembly: Ala, Asp, Glu, Gly, Ile, Leu, Lys, Ser and Val residues of phage Fd subunits. *Biochemistry* 38:4018–4027
- Overman SA, Aubrey KL, Vispo NS, Cesareni G, Thomas GJ Jr (1994) Novel tyrosine markers in Raman spectra of wild-type and mutant (Y21M and Y24M) *Ff* virions indicate unusual environments for coat protein phenoxyls. *Biochemistry* 33:1037–1042
- Robertson A D, Murphy KP (1997) Protein structure and the energetics of protein stability. *Chem Rev* 97:1251–1267
- Stetter KO, Fiala G, Huber G, Huber R, Segerer A (1990) Hyperthermophilic microorganisms. *FEMS Microbiol Rev* 75:117–124
- Sugeta H (1973) Normal vibrations and molecular conformations of dialkyl disulfides. *Spectrochim Acta A* 31:1729–1737
- Sugeta H, Go A, Miyazawa T (1973) Vibrational spectra and molecular conformations of dialkyl disulfides. *Bull Chem Soc Jpn* 46:3407–3411
- Tsuboi M, Suzuki M, Overman SA, Thomas GJ Jr (2000) Intensity of the polarized Raman band at  $1340\text{--}1345\text{ cm}^{-1}$  as an indicator of protein  $\alpha$ -helix orientation: application to Pfl filamentous virus. *Biochemistry* 39:2677–2684
- Tu AT (ed) (1982) Raman spectroscopy in biology. Wiley, New York, chap 3
- Tuma R, Russell M, Rosendahl M, Thomas GJ Jr (1995) Solution conformation of the extracellular domain of the human tumor necrosis factor receptor probed by Raman and UV-resonance Raman spectroscopy: structural effects of an engineered PEG linker. *Biochemistry* 34:15150–15156
- Vetriani C, Maeder DL, Tolliday N, Yip KS, Stillman TJ, Britton KL, Rice DW, Klump HH, Robb FT (1998) Protein thermostability above  $100^\circ\text{C}$ : a key role for ionic interactions. *Proc Natl Acad Sci USA* 95:12300–12305
- Wagner G, Braun W, Havel TF, Schaumann T, Go N, Wüthrich K (1987) Protein structures in solution by nuclear magnetic resonance and distance geometry. The polypeptide fold of the basic pancreatic trypsin inhibitor determined using two different algorithms, DISGEO and DISMAN. *J Mol Biol* 196:611–639
- Wang KY, Cho CS, Kim SS, Sung HC, Yu YG, Cho Y (1999) Structure and mechanism of glutamate racemase from *Aquifex pyrophilus*. *Nat Struct Biol* 6:422–426
- Williams W (1983) Estimation of protein secondary structure from laser Raman amide I spectrum. *J Mol Biol* 166:581–603
- Williams W, Dunker AK (1981) Determination of the secondary structure of proteins from the amide I band of the laser Raman spectrum. *J Mol Biol* 152:783–813